

# Novel Sorbicillin Derivatives with an Unprecedented Carbon Skeleton from the Sponge-Derived Fungus *Trichoderma* Species

Kerstin Neumann,<sup>[a]</sup> Ahmed Abdel-Lateff,<sup>[a]</sup> Anthony D. Wright,<sup>[b]</sup> Stefan Kehraus,<sup>[a]</sup>  
Anja Krick,<sup>[a]</sup> and Gabriele M. König\*<sup>[a]</sup>

**Keywords:** Natural products / Sorbicillin derivatives / Structure elucidation / Trichodermanones / Configuration determination

Chemical investigation of the fungus *Trichoderma* sp., isolated from the Caribbean sponge *Agelas dispar* led to four novel sorbicillinoid polyketide derivatives (**1–4**) with an unprecedented tricyclic ring system. The structures of all compounds, including the absolute configuration, were deter-

mined by interpretation of their spectroscopic data (1D and 2D NMR, CD, MS, UV and IR), and molecular modeling calculations.

(© Wiley-VCH Verlag GmbH & Co. KGaA, 69451 Weinheim, Germany, 2007)

## Introduction

Marine micro-organisms, particularly marine fungi, have been recognized as a valuable source of novel bioactive metabolites.<sup>[1–3]</sup> In this context, fungi associated with sponges were found to yield a wide variety of structural types, e.g., microsphaeropsin, pycnidione and ulocladol.<sup>[4]</sup>

Fungi of the genus *Trichoderma* are widespread in terrestrial and marine environments,<sup>[5]</sup> e.g., soil, barks, and also live in association with higher plants and sponges.<sup>[6]</sup> *Trichoderma* spp. are noted for their diverse secondary metabolite chemistry that is not characterised by any clear pattern concerning the structural types encountered. To date, around 500 compounds have been reported from fungi belonging to this genus, including the bicyclic dodecanone koniginin G,<sup>[7]</sup> the carotane derivatives trichocaranes A–D,<sup>[8]</sup> and the cyclopentenones pentenocins A and B.<sup>[9]</sup>

The current secondary metabolite investigation was focused on a marine *Trichoderma* sp., isolated from the Caribbean sponge *Agelas dispar*, collected from waters around the Island of Dominica, Windward Islands. The fungus was cultivated on a solid glucose biomalt medium containing artificial sea water (ASW). Successive fractionation of the ethyl acetate extract by vacuum liquid chromatography (VLC) and HPLC yielded four novel sorbicillinoid polyketide derivatives, compounds **1–4**, the known sorbicillinoid monomer vertinolide (**5**),<sup>[10]</sup> the dimers trichodimerol (**6**),<sup>[5,11]</sup> bislongiquinolide (**7**),<sup>[6]</sup> bisvertinol (**8**),<sup>[12]</sup> and the monomer rezishanone C (**9**), a possible product of a Diels–Alder reaction between sorbicillinol and a dienophile not related to the sorbicillinoids (Figure 1).<sup>[13]</sup>

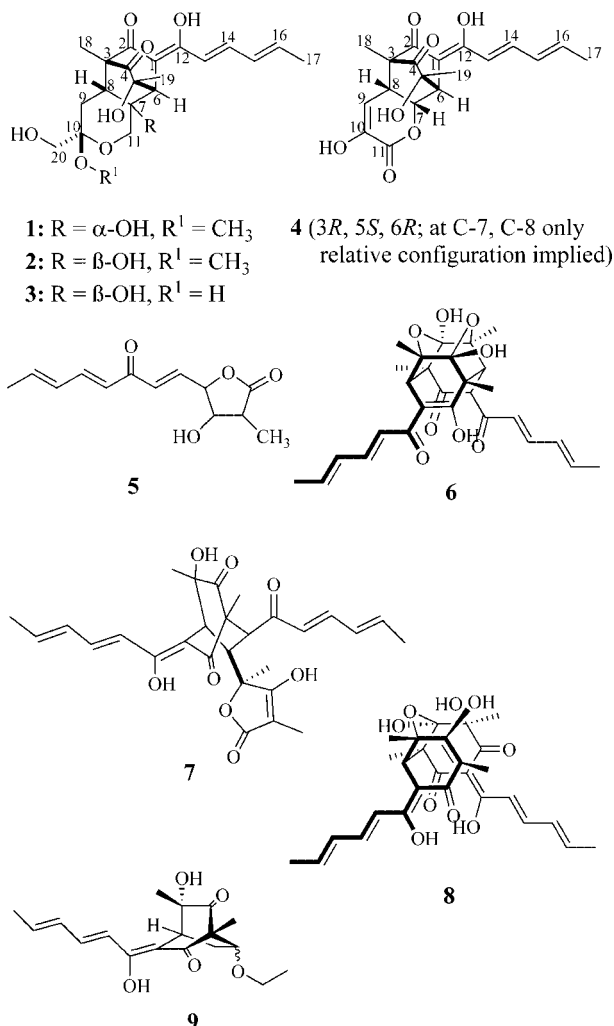


Figure 1. Compounds isolated from *Trichoderma* sp.

[a] Institute for Pharmaceutical Biology, University of Bonn, Nussallee 6, 53115 Bonn, Germany  
E-mail: g.koenig@uni-bonn.de

[b] Australian Institute of Marine Science, PMB No. 3, Townsville MC, Qld 4810, Australia

Sorbicillins are structurally unusual natural products and were discovered from several species of marine and terrestrial fungi, namely *Trichoderma* spp., *Verticillium* spp., and *Penicillium* spp.<sup>[14]</sup> This class of hexaketides and dimers thereof have been found to exhibit a broad range of biological activities including inhibition of lipopolysaccharide-induced production of tumor necrosis factor alpha (TNF- $\alpha$ ) in human monocytes,<sup>[15]</sup> radical scavenging<sup>[16]</sup> and cytotoxicity.<sup>[17]</sup>

## Results

Accurate mass measurement and  $^1\text{H}$  and  $^{13}\text{C}$  NMR analysis of compound **1** showed it to have the molecular formula  $\text{C}_{21}\text{H}_{28}\text{O}_8$ . Its  $^{13}\text{C}$  NMR spectroscopic data allowed five of the eight elements of double-bond unsaturation to be attributed to three carbon-carbon double bonds and two carbonyl groups (Table 1); the molecule thus had to be tricyclic.  $^1\text{H}$  and  $^{13}\text{C}$  NMR spectra showed the presence of two  $\text{sp}^3$  hybridized methine groups, four  $\text{sp}^2$  hybridized methine groups, three methylene groups, two of them attached to oxygen, one allylic methyl group, two methyl groups attached to quaternary carbons, one methoxyl group and eight quaternary carbons. The NMR spectroscopic data further enabled all but four hydrogen atoms of **1** to be attached to carbons; hence it was evident that the remaining four are present in the molecule as hydroxyl functions, a deduction supported by IR data ( $\tilde{\nu}_{\text{max}} = 3315\text{ cm}^{-1}$ ). One of them was assigned in the  $^1\text{H}$  NMR spectrum to the resonance at  $\delta = 14.2$ , and showing it to probably hydrogen-bond to a keto-function.

The planar structure of **1** was deduced by interpretation of its  $^1\text{H}$ - $^1\text{H}$  COSY and  $^1\text{H}$ - $^{13}\text{C}$  HMBC 2D shift correlated

NMR spectroscopic data. Initially, four partial substructures were deduced (Figure 2). Fragment 1, a sorbyl unit, was elucidated based on a  $^1\text{H}$ - $^1\text{H}$  spin system from 17- $\text{H}_3$  to 13- $\text{H}$ , as well as  $^1\text{H}$ - $^{13}\text{C}$  long range correlations between 13- $\text{H}$  and C-12. The chemical shift of C-12 ( $\delta_{\text{C}} = 167.8\text{ ppm}$ ) evidenced this carbon to bear a hydroxy group. Fragment 2 (ring A) was characterised by the presence of many quaternary carbons. Heteronuclear long range couplings were observed from the resonance of 6- $\text{H}$  to those of C-1, C-2, C-4 and C-5, between 19- $\text{H}_3$  and C-4, C-5 and C-6, and between 18- $\text{H}_3$  and C-2, C-3 and C-4, and evidenced these methyl groups to be bonded to C-5 and C-3, respectively. These correlations also made clear that C-5 was bonded to C-6 and C-4, and C-3 to C-2 and C-4. The chemical shifts for C-2 and C-4 in the  $^{13}\text{C}$  NMR spectrum of **1** placed the carbonyl functionalities at these positions, while C-1 was part of a carbon-carbon double bond and C-5 hydroxylated. From the spectroscopic data it was evident that fragment 3 (ring B) partly overlapped with fragment 2, i.e., concerning C-3, C-4, C-5 and C-6. Long range C-H correlations between the resonances of 8- $\text{H}$  and C-3 implied that C-8 is directly bonded to C-3, and C-7 is located next to C-6 because of HMBC correlations between 6- $\text{H}$  and C-7. According to its characteristic chemical shift, C-7 ( $\delta_{\text{C}} = 92.7\text{ ppm}$ ) must also bear a hydroxy group. For fragment 4 (ring C), proton-proton couplings between 8- $\text{H}$  and 9- $\text{ax}$ - $\text{H}$  proved that C-8 has to be bonded directly to C-9. The latter carbon is linked to C-10 based on HMBC couplings observed between 9- $\text{H}_2$  and C-10. Long range correlations between 20- $\text{H}_2$  and C-9 and C-10 then led to the linkage between C-10 and the hydroxy methylene functionality being established. The  $^{13}\text{C}$  NMR chemical shifts of C-10 ( $\delta = 110.6\text{ ppm}$ , s) and C-11 ( $\delta = 69.7\text{ ppm}$ , t) indicated C-10 to

Table 1. NMR spectroscopic data of **1** measured in  $[\text{D}_6]\text{acetone}$  at 300 and 500 MHz.

Position	$\delta_{\text{C}}$ in ppm	$\delta_{\text{H}}$ in ppm, mult., $J$ (Hz)	$^1\text{H}$ - $^1\text{H}$ COSY correlations	HMBC correlations	NOE correlations
1	112.3 C				
2	199.0 C				
3	64.1 C				
4	210.9 C				
5	74.7 C				
6	49.1 CH	3.38, s		1, 2, 4, 5, 7, 8, 12	11 <sub>eq</sub> , 13, 19
7	92.7 C				
8	50.2 CH	2.56, d, 10.7	9 <sub>ax</sub>	2, 3, 4, 9, 10, 11	9 <sub>eq</sub> , 11 <sub>ax</sub> , 18
9	38.1 CH <sub>2</sub>	ax: 2.64, dd, 10.7, 13.6 eq: 1.75, d, 13.6	8, 9 <sub>eq</sub> 8, 9 <sub>ax</sub>	3, 7, 8, 10 3, 7, 8, 10	8, 9 <sub>eq</sub> , 20 <sub>a</sub> 8, 9 <sub>ax</sub> , 18
10	110.6 C				
11	69.7 CH <sub>2</sub>	ax: 4.35, d, 11.8 eq: 3.71, d, 11.8	6, 11 <sub>eq</sub> 11 <sub>ax</sub>	7, 8	8, 11 <sub>eq</sub> , 21 6, 11 <sub>ax</sub>
12	167.8 C				
13	120.4 CH	6.57, d, 15.0	14, 15	1, 12, 14, 15	6, 14, 15, 19
14	141.4 CH	7.22, dd, 10.9, 15.0	13, 15, 16, 17	12, 16	13, 15, 16
15	132.1 CH	6.38, dd, 10.9, 15.0	13, 14, 16	16, 17	13, 14, 16, 17
16	138.7 CH	6.18, dq, 15.0, 6.8	13, 15, 17	14, 15, 17	14, 17
17	18.8 CH <sub>3</sub>	1.80, d, 6.8	13, 15, 16	15, 16	15, 16
18	10.9 CH <sub>3</sub>	1.10, s	8, 9 <sub>ax</sub>	2, 3, 4, 8	8, 9 <sub>ax</sub>
19	27.0 CH <sub>3</sub>	1.14, s		4, 5, 6	6, 13
20	62.7 CH <sub>2</sub>	a: 3.82, d, 10.9 b: 3.40, d, 10.9	20 <sub>b</sub> 20 <sub>a</sub>	9, 10	9 <sub>eq</sub> , 11 <sub>eq</sub> , 20 <sub>b</sub> , 21 9 <sub>eq</sub> , 11 <sub>eq</sub> , 20 <sub>a</sub>
21	48.8 CH <sub>3</sub>	2.98, s		10	20 <sub>a</sub> , 20 <sub>b</sub> , 11 <sub>ax</sub>
12-OH		14.20, s			

be attached to two and C-11 to one oxygen atom. One of these oxygens connected to C-10 proved to be part of the methoxyl group C-21, based on the diagnostic long range correlation observed between the resonances of 21-H<sub>3</sub> and C-10. Subsequently, C-10 and C-11 were concluded to be connected via an ether bridge. Finally, long range correlations observed between the resonances of 11-H and C-7 showed C-11 to be attached directly to C-7, completing ring C. Applying the ACD/Chem. Sketch software,<sup>[18]</sup> the calculated <sup>1</sup>H and <sup>13</sup>C NMR shifts for fragments 2, 3 and especially 4 were found to be in good accordance to the experimental data and strengthened the suggestion of an ether functionality between C-10 and C-11. Fragments 1 to 4 were then connected making use of further HMBC correlations. Heteronuclear couplings between 6-H and C-12 and between 13-H and C-1 proved that fragment 1 attached to fragment 2 via C-1. Extension of fragment 2 was achieved by connecting C-6 to C-7 and C-3 to C-8 (shown in fragment 3), and results in a bridged ring system composed of rings A and B. Fragments 3 and 4 must then be linked via C-7 and C-8, since these carbons are common to both substructures. Further proof for this structural assignment came from long range <sup>1</sup>H-<sup>1</sup>H spin couplings between 11-H<sub>2</sub> and 6-H and between 18-H<sub>3</sub> and 9-H<sub>2</sub>.

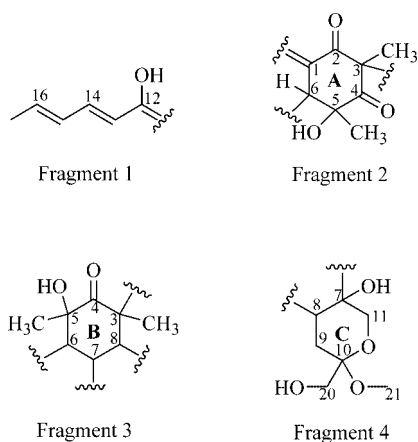


Figure 2. Fragments of Compound **1** deduced from NMR spectroscopic data.

2D NOESY and selective gradient NOE data, energy-minimized 3D models and proton coupling constant analysis and calculations, as well as CD measurements were used to assign the absolute configuration. First the sorbicillin part of the molecule was investigated. The bridged ring system consisting of rings A and B is only possible if 6-H and 18-CH<sub>3</sub> are disposed equatorially. NOE enhancements of 13-H and 6-H were observed by irradiation of 19-H<sub>3</sub>, showing the C-19 methyl group to be oriented towards the sorbyl side chain. With this information, the relative configuration of this part of the molecule was designated as 3*R*\*, 5*S*\*, 6*R*\*. A CD spectrum of **1** gave proof for the (3*R*,5*S*,6*R*) absolute configuration of the molecule. Characteristic Cotton effects with a minimum at 295 nm and a maximum at 335 nm were observed that corresponded well with those

reported for rezishanone C,<sup>[13]</sup> which contains a similar sorbicillin-substructure to the one reported here.

Selective NOE experiments also proved to be helpful for deducing the configuration of the non-sorbicillin part of **1**. NOE enhancements observed for 8-H and of 21-CH<sub>3</sub> upon irradiation of the 11<sub>ax</sub>-H resonance ( $\delta = 4.35$  ppm) indicated the methoxyl group and 8-H to have axial orientation, and to be located on the same side of the molecule. Consequently, 11-H ( $\delta = 3.71$  ppm) must have equatorial orientation, a finding that also explains the enhancement of 6-H by irradiation of 11<sub>eq</sub>-H ( $\delta = 3.71$  ppm). Ring C thus adopts a chair conformation.

Still missing at this point was information concerning the relative configuration at C-7. Furthermore, the relative configuration of ring A (C-3, C-5 and C-6) could not yet be related to that of ring C (C-7, C-8, C-10). NOE experiments were not useful in this case due to the quaternary nature of C-7. It was suspected however that the conformation of ring C and thus <sup>1</sup>H-<sup>1</sup>H coupling constants were dependent on the configuration at C-7. The magnitude of proton-proton coupling constants deduced from <sup>1</sup>H NMR experiments were thus considered and compared with those obtained from molecular modeling calculations. It was clear from the large coupling constant measured for *J*<sub>8/9<sub>ax</sub></sub> (10.7 Hz) that, according to the Karplus equation,<sup>[18–20]</sup> these two protons must have a torsion angle of close to 180°. The absence of <sup>1</sup>H-<sup>1</sup>H couplings between 8-H and 9<sub>eq</sub>-H indicated the dihedral angle between these two protons to be close to 90°. Four models were calculated for compound **1** taking into account all possible configurations at C-7, C-8 and C-10; i.e. (7*R*,8*R*,10*S*), (7*S*,8*R*,10*S*), (7*S*,8*S*,10*R*) and (7*R*,8*S*,10*R*), with configurations at C-3, C-5 and C-6 taken as *R*, *S* and *R*, respectively (see Figure 3, parts a–d). Model #4, having (7*R*,8*S*,10*R*) configuration, was considered not appropriate, as ring C does not have the required chair conformation. When comparing the remaining models that all displayed ring C in a chair conformation, a significant difference was noted concerning the size of the dihedral angles

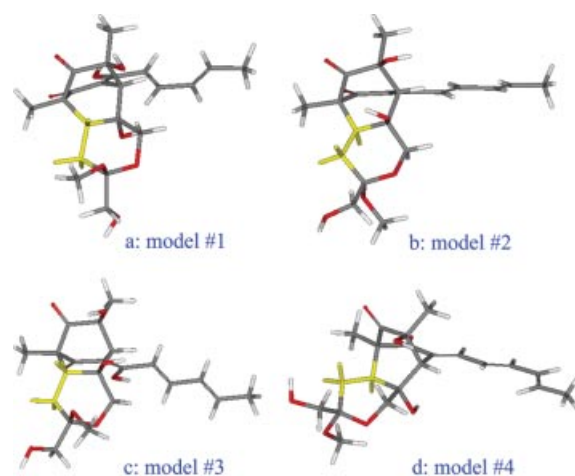


Figure 3. a–d. Minimum energy conformation of epimers of **1**. Model #1: (7*R*,8*R*); model #2: (7*S*,8*R*); model #3: (7*S*,8*S*); model #4: (7*R*,8*S*).

Table 2. Calculated  $^1\text{H}$ - $^1\text{H}$  coupling constants for models #1–4 and measured coupling constants for compounds **1**–**3**.<sup>[a]</sup>

	Torsion angle	Coupling constant calculated (Hz)		Compound	Coupling constant measured (Hz)	
Model #1	8-H/ $9_{\text{eq}}$ -H	78.6°	1.2	<b>1</b>	8-H/ $9_{\text{eq}}$ -H	0.0
	8-H/ $9_{\text{ax}}$ -H	171.4°	12.1		8-H/ $9_{\text{ax}}$ -H	10.7
Model #2	8-H/ $9_{\text{eq}}$ -H	29.3°	8.0	<b>2</b>	8-H/ $9_{\text{eq}}$ -H	7.3
	8-H/ $9_{\text{ax}}$ -H	145.8°	9.1		8-H/ $9_{\text{ax}}$ -H	9.9
Model #3	8-H/ $9_{\text{eq}}$ -H	62.0°	2.7	<b>3</b>	8-H/ $9_{\text{eq}}$ -H	7.0
	8-H/ $9_{\text{ax}}$ -H	179.8°	12.4		8-H/ $9_{\text{ax}}$ -H	9.9
Model #4	8-H/ $9_{\text{eq}}$ -H	45.3°	5.3			
	8-H/ $9_{\text{ax}}$ -H	160.8°	11.3			

[a] Implied configuration for all models is (3*R*,5*S*,6*R*).

between 8-H and  $9_{\text{ax}}$ -H/ $9_{\text{eq}}$ -H. These torsion angles were calculated for the minimized structures #1 to #3 and used in the Karplus equation to calculate the expected  $^1\text{H}$ - $^1\text{H}$  coupling constants.<sup>[20,21]</sup> As shown in Table 2, the calculated coupling constants for the minimized (7*R*,8*R*,10*S*) epimer corresponded best with the actual NMR values and thus led to the conclusion that **1** possesses a *trans*-junction between the sorbicillin part and the non-sorbicillin part of the molecule, with the hydroxy group at C-7 having an  $\alpha$  orientation. Based on this evidence, the absolute configuration of **1** is proposed as (3*R*,5*S*,6*R*,7*R*,8*R*,10*S*). For **1**, the trivial name trichodermanone A is proposed.

Mass spectral analysis of **2** showed it to have the same molecular formula as **1**. Analysis of its NMR spectroscopic data, in particular the  $^1\text{H}$ - $^1\text{H}$  COSY and  $^1\text{H}$ - $^{13}\text{C}$  HMBC spectroscopic data, revealed **2** and **1** to have identical planar structures meaning the two molecules must differ in configuration at one or more of their chiral centers. NOE correlations for **2** were observed between 6-H, 13-H and 19-H<sub>3</sub> as in **1**. A CD spectrum of **2** showed it to be almost congruent to that measured for **1**, proving the configuration in the sorbicillin part of the molecule to be the same as for **1**. Ring C of **2** must also have a chair conformation due to mutual NOE enhancements of 21-H<sub>3</sub> and 8-H with 11-H<sub>2</sub>, respectively. Irradiation of 8-H caused enhancements of both  $9_{\text{ax}}$ -H ( $\delta$  = 2.17 ppm) and  $9_{\text{eq}}$ -H ( $\delta$  = 1.69 ppm), indicating that the torsion angles between 8-H and the protons at C-9 are different from those in **1**. The proton coupling constants measured for  $J_{8/9_{\text{ax}}}$  (9.9 Hz) and  $J_{8/9_{\text{eq}}}$  (7.3 Hz) confirmed this deduction. With this information in hand the measured  $^1\text{H}$ - $^1\text{H}$  coupling constants of **2** were compared to those calculated for models #1 to #3 (Table 2). The actual coupling constants obtained by experimental measurement were almost identical to those calculated for model #2, that has a *cis*-junction of rings B and C, and C-7 and C-8 having *S* and *R* absolute configurations, respectively. For **2** the absolute configuration of (3*R*,5*S*,6*R*,7*S*,8*R*,10*S*), and the trivial name trichodermanone B are proposed.

The molecular formula and NMR spectroscopic data of **3** revealed it to have the same planar structure as **2** except for the functionality at C-10, being -OCH<sub>3</sub> in **2** and -OH in **3**. The  $^{13}\text{C}$  NMR spectroscopic data for the two compounds

were almost identical with the exception of the resonance frequencies associated with C-10 and C-20. The configuration of the sorbicillin part of the molecule was solved by taking the mutual NOE correlations between 6-H, 13-H and 19-H<sub>3</sub> into account, and by comparison of the CD spectra of **3** with those of **1** and **2**, and found to be as shown in **3**. The mutual NOE correlations observed between 8-H and  $11_{\text{ax}}$ -H indicated ring C to have a chair conformation, similar to that found in **1** and **2**. Calculation of the  $^1\text{H}$ - $^1\text{H}$  coupling constants for  $J_{8/9_{\text{ax}}}$  and  $J_{8/9_{\text{eq}}}$  yielded values comparable to those measured for model #2, showing that **3** has a *cis* junction between rings B and C, leading to the absolute configuration of **3** being best described as (3*R*,5*S*,6*R*,7*S*,8*R*,10*S*). The trivial name trichodermanone C is proposed for **3**.

Mass spectral analysis of **4** showed it to have the molecular formula C<sub>19</sub>H<sub>20</sub>O<sub>7</sub>. Extensive comparison of  $^1\text{H}$ ,  $^{13}\text{C}$ ,  $^1\text{H}$ - $^1\text{H}$  COSY, and  $^1\text{H}$ - $^{13}\text{C}$  HMBC NMR spectroscopic data of **1** and **2** with those of **4** showed that the data were in good agreement concerning the sorbyl unit, and rings A and B. Differences between the compounds were, however, evident from the spectroscopic data associated with ring C. From  $^1\text{H}$ - $^1\text{H}$  COSY correlations observed between 8-H and 9-H, and the HMBC couplings observed between 9-H and C-8, it was clear that C-9 had to be attached to C-8. HMBC couplings between 9-H and C-10 and C-11 enabled the C–C bond from C-9 to C-10 to be established. Linkage between C-7 and C-11 via an oxygen and the completion of ring C was probable taking into account the  $^{13}\text{C}$  NMR shift of C-7 ( $\delta$  = 80.9, d), which clearly differs from the equivalent atom in **2** ( $\delta$  = 90.3, s). Comparison of the NOESY correlations and the CD spectra of **2** and **4** showed the configuration for this pair of molecules to be the same for the stereogenic centers C-3, C-5 and C-6; (3*R*,5*S*,6*R*). The large  $^1\text{H}$ - $^1\text{H}$  NMR coupling constants associated with 8-H and 7-H ( $J_{\text{H}7,\text{H}8}$  = 10.6 Hz) showed these protons to have either a dihedral angle of about 180° or close to 0°; mutual NOESY correlations between 8-H and 7-H revealed the angle to be close to 0° meaning the junction between rings B and C had to be *cis*. In order to obtain information on the absolute configurations at C-7 and C-8, molecular modeling experiments with the two possible isomers – 7*S*,8*R* and

7*R*,8*S* – were performed. The two models unfortunately did not show significant differences in the torsion angles for 7-*H* and 8-*H* and so the absolute configuration of **4** remains unresolved.

## Discussion

Natural products belonging to the sorbicillin class are hexaketide-derived metabolites. All of these compounds are composed of a cyclohexanone ring to which a sorbyl, i.e. hexa-2,4 dien-one, chain is attached. Structural variations within this structural class concern the substitution of the cyclohexanone ring, which often is further methylated and hydroxylated. The sorbyl side chain, however in most cases remains unchanged with exception of a few 2,3-dihydrosorbyl-derivatives.<sup>[13]</sup> More than 30 different sorbicillin monomers have been found to date: For the recently published rezishanones it is postulated that they originate from sorbicillinol (**10**) and butylvinyl or ethylvinyl ethers attached to **10** via a Diels–Alder reaction.<sup>[13]</sup> The only known nitrogen-containing sorbicillinoids are the anti-cancer agents sorbicillactone A and B, whose biosynthesis also involves sorbicillinol (**10**), the amino acid alanine and presumably a fumaryl-related C<sub>4</sub> unit.<sup>[17]</sup> Sorbicillinol itself was also shown to

be the common precursor for many dimeric sorbicillin derivatives giving rise to a high structural diversity within this group of natural products.<sup>[10]</sup> The dimers are biosynthetically generated from **10** through two ways of dimerization, i.e. Diels–Alder cycloaddition, as in the case of bisorbicillinol,<sup>[22]</sup> and Michael addition, as suggested for trichodimerol.<sup>[23]</sup>

Compounds **1–4**, even though sharing the basic sorbicillin part of their structures with that of other sorbicillinoids, possess an unprecedented tricyclic ring system. They are unique with regard to ring C, which may arise biosynthetically by combining a non-sorbicillinoid polyketide with the hexaketide-derived sorbicillinol. A biosynthetic pathway proposed for compounds **1–4** is shown in Figure 4. Our proposal is similar to that of Trifonov et al. for the bisvertinols concerning the first steps of biosynthesis up to the formation of **10**.<sup>[12]</sup> In their concept all known sorbicillinoid structures derive from 2,4-dimethyldodecyl units yielding sorbicillin, an assumption confirmed by Abe et al. via biosynthetic studies with labeled acetate units.<sup>[24]</sup> According to Trifonov et al. sorbicillin undergoes an epoxidation, a process also proposed as a key step in the biosynthesis of penicillic acid from orsellinic acid.<sup>[25]</sup> Opening of the epoxide ring would then lead to the quinol sorbicillinol (**10**). It is

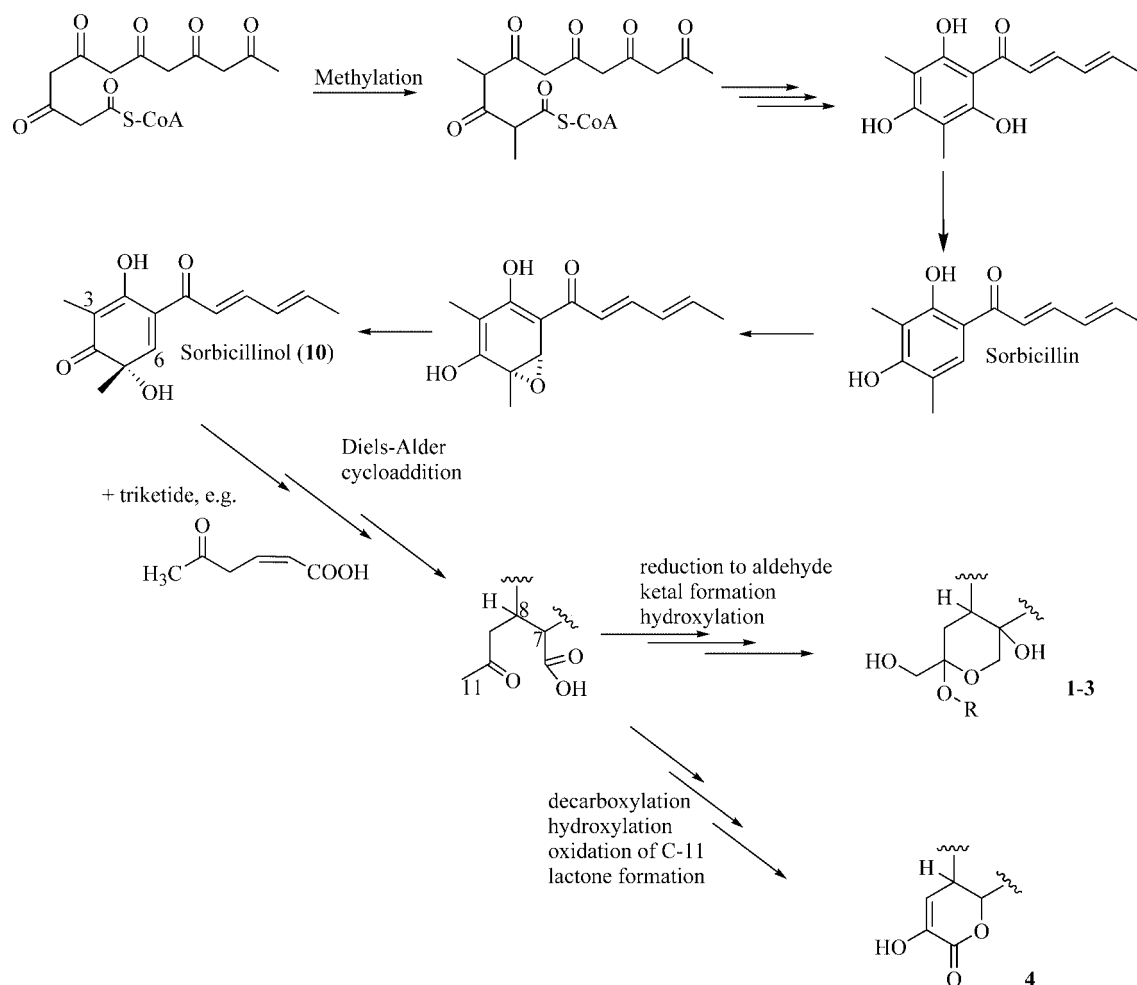


Figure 4. Proposed biosynthetic pathway for compounds **1–4**.



probable that compounds **1–4** were produced from **10** via a Diels–Alder cycloaddition of another polyketide, followed by cyclization and hydroxylation to give compounds **1–3**, or oxidation and decarboxylation to yield compound **4** (see Figure 4). This combination of two polyketide precursors for the formation of secondary metabolites is especially exciting, as this is a very rare case in nature.

Compounds **1–3** were tested in variety of bioassays including agar diffusion tests for antimicrobial properties, tests for antiparasitic and cytotoxic activity, phosphatase inhibiting activity, acetylcholine esterase inhibition and trypsin inhibition. In each case no activity was observed for the tested compound. Moderate activity was found in the 1,1-diphenyl-2-picrylhydrazyl radical scavenging activity test (DPPH test), which is in agreement to published data for other sorbicillin derivatives.<sup>[11]</sup> Due to the small amount of **4** obtained during isolation it was not tested in any of the assays.

## Experimental Section

**General Procedure:** HPLC was carried out using a Merck–Hitachi system equipped with a L-6200A intelligent pump, a L-4500 photodiode array detector, a D-6000 interface with a D-7000 HSM software, and a Rheodyne 7725i injection system. UV and IR spectra were obtained using Perkin–Elmer Lambda 40 and Perkin–Elmer Spectrum BX instruments, respectively. Optical rotations were recorded on a Jasco DIP 140 polarimeter. HREIMS was measured on a Kratos MS 50 spectrometer. LC-ESIMS was performed using an API 2000, LC MS/MS from Applied Biosystems/MDS Sciex. All NMR spectra were recorded on Bruker Avance 300 DPX and 500 DRX spectrometers in (CD<sub>3</sub>)<sub>2</sub>CO. Spectra were referenced to residual solvent signals with resonances at  $\delta_{H/C}$  2.04/29.8 [(CD<sub>3</sub>)<sub>2</sub>CO]. CD spectra have been recorded on an AVIV 62DS circular dichroism spectrometer in methanol at room temperature. The concentrations of all samples were  $2.5 \times 10^{-3}$  mol L<sup>-1</sup>, the path length was  $d = 0.05$  cm. A background correction was performed by subtracting the spectrum of the neat solvent recorded under identical conditions.

**Isolation and Taxonomy of the Fungal Strain:** The sponge *Agelas dispar* J. was collected in December–January of 1993 by divers using SCUBA from the waters around the Caribbean Island of Dominica. The sponge was identified by Dr. R. Desqueroix-Faundez, Musée d'Histoire Naturelle, Geneva. The fungus was isolated by inoculating small pieces of the sponge's inner tissue onto a medium containing cellulose (10 g/L), yeast extract (1 g/L), benzylpenicillin (250 mg/L), streptomycin sulfate (250 mg/L), agar (15 g/L) and ASW (800 mL/L). Artificial sea water (ASW) contained the following salts (g/L): KBr (0.1), NaCl (23.48), MgCl<sub>2</sub>·6H<sub>2</sub>O (10.61), CaCl<sub>2</sub>·6H<sub>2</sub>O (1.47), KCl (0.66), SrCl<sub>2</sub>·6H<sub>2</sub>O (0.04), Na<sub>2</sub>SO<sub>4</sub> (3.92), NaHCO<sub>3</sub> (0.19), H<sub>3</sub>BO<sub>3</sub> (0.03).<sup>[18]</sup> The fungal strain was identified as belonging to the genus *Trichoderma* by Dr. S. Draeger, Institute for Microbiology, Technical University of Braunschweig.

**Cultivation:** The fungus was cultivated at room temperature for two months in 5.75 L (23 Fernbach flasks) of solid medium containing 50 g/L biomalt (Villa Natura Gesundheitsprodukte GmbH, Germany), 10 g/L glucose (J. T. Baker), 15 g/L agar (Fluka Chemie AG) in artificial sea water (ASW).

**Extraction and Isolation:** Mycelia and medium were homogenized using an Ika Ultra-Turrax at 8000 rpm. The resulting mixture was exhaustively extracted with EtOAc (3 × 6 L) and filtered. The filtrate was evaporated to yield 2.5 g of a yellowish brown crude extract. This extract was fractionated by reversed phase vacuum liquid chromatography (RP-VLC) (2.5 × 20 cm, RP C-18 material, 70 g), employing gradient elution from 10:90 H<sub>2</sub>O/MeOH to MeOH, to yield 9 fractions. According to the differences in composition of the fractions as detected by <sup>1</sup>H-NMR spectroscopy, especially with respect to several low-field resonances in the  $\delta = 6–8$  region, fractions 4, 5 and 6 seemed promising for further investigation. These three fractions were combined and fractionated by NP-VLC (2 × 15 cm, Si gel 60, 30 g, Merck 7739), using gradient elution from petroleum ether to EtOAc, followed by MeOH, to yield 15 fractions. Fraction 4.6.4 gave a very prominent single spot on TLC and was subjected to further spectroscopic investigation without further purification. The spectroscopic data revealed the compound to be pure **9** (24 mg). Fraction 4.6.5 yielded 32.0 mg of semi-pure **6**. Fractions 4.6.7 and 4.6.8 were combined and subjected to RP-18 HPLC (eluent 65:35 MeOH/H<sub>2</sub>O), to yield 7 fractions that were further purified by HPLC [eluent 50:25:25 petroleum ether/(CH<sub>3</sub>)<sub>2</sub>CO/EtOAc], to yield 14 mg of **2** ( $t_R = 9$  min).

Compounds **1** (5.2 mg,  $t_R = 37$  min) and **3** (11.9 mg,  $t_R = 27$  min) were purified from fraction 4.6.9, after two RP-18 HPLC separations (eluent 60:40 MeOH/H<sub>2</sub>O for the first and 45:55 MeOH/H<sub>2</sub>O for the second HPLC). From fraction 4.6.9 we also isolated 11.5 mg of semi-pure compound **5** ( $t_R = 30.4$  min).

The extract from a second cultivation of the fungus, was fractionated by VLC (2.5 × 20 cm, Si gel 60, 120 g, Merck 7739), employing a gradient elution from petroleum ether to (CH<sub>3</sub>)<sub>2</sub>CO, to yield 5 fractions [petroleum ether/(CH<sub>3</sub>)<sub>2</sub>CO 1:0, 7.5:2.5, 5:5, 2.5:7.5, 0:1, 200 mL each]. According to the low field resonances in the  $\delta = 6–8$  region of the <sup>1</sup>H NMR spectroscopic data, fractions 2 and 3 were further investigated. VLC fraction 3 was fractionated over NP-Si (5–40  $\mu$ m, Merck 7739) by VLC employing gradient elution from petroleum ether to EtOAc, to yield 11 fractions (petroleum ether/EtOAc = 1:0, 9:1, 8:2, 7:3, 6:4, 5:5, 4:6, 3:7, 2:8, 1:9, 0:1; 10 mL each). Fraction 3.4 was then purified by RP-18 HPLC (Eurospher-100, 5  $\mu$ m, 250 × 8 mm ID, Knauer), employing a gradient elution from 9:1 H<sub>2</sub>O/MeOH to MeOH in 45 min, 2 mL/min, to yield **5** ( $t_R = 32$  min, 4 mg) and semi-pure **7** ( $t_R = 41$  min). Compound **7** was then purified by gradient elution from 1:1 H<sub>2</sub>O/MeOH to MeOH in 45 min, 2 mL/min ( $t_R = 29$  min, 4 mg). Fraction 3.6 was purified by RP-18 HPLC (Eurospher-100, 5  $\mu$ m, 250 × 8 mm ID, Knauer), using a gradient of 6:4 H<sub>2</sub>O/MeOH to MeOH in 60 min, 2 mL/min, and yielded four fractions (3.6.4–3.6.7;  $t_R = 25$  min, 26 min, 29 min, 35 min, respectively). The first of these fractions was purified using RP-HPLC (XTerra RP-18, 5  $\mu$ m, 250 × 4.6 mm, Waters), employing a gradient elution from 65:35 H<sub>2</sub>O/MeOH to MeOH in 35 min, 1 mL/min, to give 10 mg of **3** ( $t_R = 21$  min) and 2 mg of **4** ( $t_R = 25$  min). HPLC peak 3.6.5 was purified using RP-18 HPLC (gradient elution 65:35 H<sub>2</sub>O/MeOH to 20:80 H<sub>2</sub>O/MeOH in 35 min, 1 mL/min) to yield 4 mg of **2** ( $t_R = 22$  min), and 1 mg of **3** ( $t_R = 21$  min). HPLC peak 3.6.6 was further purified employing RP-18 HPLC (gradient elution from 7:3 H<sub>2</sub>O/MeOH to 3:7 H<sub>2</sub>O/MeOH in 30 min, 1 mL/min) to yield 4 mg of **1** ( $t_R = 23.5$  min). Fraction 3.6.7 was subjected to RP-18 HPLC (Eurospher-100, 5  $\mu$ m, 250 × 8 mm ID, Knauer), using gradient elution from 55:45 H<sub>2</sub>O/MeOH to MeOH in 60 min, 2 mL/min to yield 10 mg of **3** ( $t_R = 23$  min).

VLC fraction 2 was subjected to normal phase VLC, using a gradient elution from petroleum ether to EtOAc, to yield 5 fractions

(petroleum ether/EtOAc = 1:0, 9:1, 8:2, 7:3, 6:4, 5:5, 4:6, 3:7, 2:8, 1:9, 0:1, 200 mL each). Fraction 2.4 was then purified by RP-HPLC (Eurospher-100, 5  $\mu$ m, 250  $\times$  8 mm ID, Knauer), employing gradient elution from 7:3 H<sub>2</sub>O/MeOH to MeOH in 50 min, 2 mL/min, and yielded **1** ( $t_R$  = 29 min, 2 mg), **2** ( $t_R$  = 32 min, 2 mg) and **8** ( $t_R$  = 44 min, 2 mg).

**Molecular Modeling:** All models were calculated employing conformation search (Boltzman jump) and a standard force field as implemented in the Cerius<sup>2</sup> 4.0 (MSI) molecular modeling software package. Models were further refined with 1500 iterations of minimisation. Calculations were performed using a Silicon Graphics O2 workstation (Irix 6.5.6).

**Trichodermanone A (1):** (5.2 mg); yellowish viscous oil.  $[a]_D^{25} = +203.0$  (MeOH,  $c = 0.24$ ). UV (MeOH)  $\lambda_{max}$  (log  $\epsilon$ ): 360 (4.6), 248 (4.2), 203 (4.2) nm. CD (MeOH)  $\Delta\epsilon = 335$  (+1.990), 293 (−1.945). IR (film):  $\tilde{\nu} = 3315, 2920, 2851, 1732, 1630, 1602, 1565, 1455, 1381$  cm<sup>−1</sup>. <sup>1</sup>H and <sup>13</sup>C NMR spectroscopic data see Table 1. EIMS:  $m/z$  (% rel. int.) = 408 (10) [M<sup>+</sup>], 376 (100), 101 (80), 95 (40), 59 (90), accurate mass found  $m/z$  376.1519 [M − CH<sub>2</sub>OH]<sup>+</sup> (calcd. for C<sub>20</sub>H<sub>24</sub>O<sub>7</sub>  $m/z$  376.1522).

**Trichodermanone B (2):** (14.0 mg); yellowish viscous oil.  $[a]_D^{25} = +251.0$  (MeOH,  $c = 0.2$ ). UV (MeOH)  $\lambda_{max}$  (log  $\epsilon$ ): 358 (4.7), 248 (4.2), 202 (4.4) nm. CD (MeOH)  $\Delta\epsilon = 348$  (+5.436), 310 (−6.950). IR (film):  $\tilde{\nu} = 3393, 2938, 1733, 1630, 1600, 1561, 1383$  cm<sup>−1</sup>. <sup>1</sup>H

Table 3. NMR spectroscopic data of **2** measured in [D<sub>6</sub>]acetone at 300 and 500 MHz.

Position	$\delta_C$ in ppm	$\delta_H$ in ppm, mult., $J$ (Hz)	<sup>1</sup> H- <sup>1</sup> H COSY correlations	HMBC correlations	NOE correlations
1	111.5 C				
2	200.2 C				
3	64.5 C				
4	210.9 C				
5	74.7 C				
6	49.1 CH	3.51, s		1, 2, 4, 5, 7, 8, 12	11, 13, 19
7	90.3 C				
8	49.7 CH	2.56, dd, 7.3, 9.9	9 <sub>eq</sub> , 9 <sub>ax</sub>	2, 3, 4, 9, 11, 18	9 <sub>eq</sub> , 9 <sub>ax</sub> , 11, 18
9	40.9 CH <sub>2</sub>	ax: 2.17, dd, 9.9, 13.9 eq: 1.69, dd, 7.3, 13.9	8, 9 <sub>eq</sub> 8, 9 <sub>ax</sub>	3, 8, 10, 20 3, 7, 8, 10	8, 9 <sub>eq</sub> , 18 8, 9 <sub>ax</sub> , 18
10	111.0 C				
11	68.4 CH <sub>2</sub>	3.91, br. m	20 <sub>a</sub>	6, 7	6, 8, 21
12	168.9 C				
13	120.0 CH	6.44, d, 15.0	14, 15, 16	12, 15	6, 14, 15, 16, 19
14	142.1 CH	7.25, dd, 11.0, 15.0	13, 15, 16, 17	12, 15, 16	16
15	132.0 CH	6.39, dd, 11.0, 15.0	13, 14, 16, 17	16, 17	13, 17
16	139.5 CH	6.23, dq, 15.0, 7.0	13, 15, 17	14, 15, 17	14
17	18.8 CH <sub>3</sub>	1.86, d, 7.0	13, 15, 16	13, 15, 16	15, 16
18	11.8 CH <sub>3</sub>	1.08, s	8, 9 <sub>eq</sub>	2, 3, 4, 8	8, 9 <sub>eq</sub>
19	26.5 CH <sub>3</sub>	1.14, s		4, 5, 6	6, 11, 13
20	62.2 CH <sub>2</sub>	a: 3.85, d, 11.0 b: 3.01, d, 11.0	20 <sub>b</sub> 20 <sub>a</sub>	10	9 <sub>eq</sub> , 20 <sub>b</sub> , 21 20 <sub>a</sub> , 21
21	48.9 CH <sub>3</sub>	3.20, s			11, 20 <sub>b</sub>

Table 4. NMR spectroscopic data of **3** measured in [D<sub>6</sub>]acetone at 300 and 500 MHz.

Position	$\delta_C$ in ppm	$\delta_H$ in ppm, mult., $J$ (Hz)	<sup>1</sup> H- <sup>1</sup> H COSY correlations	HMBC correlations	NOE correlations
1	111.6 C				
2	200.0 C				
3	64.4 C				
4	211.0 C				
5	74.7 C				
6	49.6 CH	3.37, s	19	1, 2, 4, 5, 7, 8, 12	11 <sub>ax</sub> , 11 <sub>eq</sub> , 13, 19
7	90.3 C				
8	49.9 CH	2.71, dd, 7.0, 9.9	9 <sub>eq</sub> , 9 <sub>ax</sub>	2, 3, 4, 9, 11, 18, 20	9 <sub>eq</sub> , 11 <sub>ax</sub> , 11 <sub>eq</sub> , 18
9	40.3 CH <sub>2</sub>	ax: 2.17, dd, 9.9, 14.1 eq: 1.74, dd, 7.0, 14.1	8, 9 <sub>eq</sub> 8, 9 <sub>ax</sub>	3, 7, 8, 10 3, 6, 8, 10	8, 9 <sub>eq</sub> 9 <sub>ax</sub> , 20
10	107.5 C				
11	68.2 CH <sub>2</sub>	ax: 4.28, d, 11.7 eq: 3.76, d, 11.7	11 <sub>eq</sub> 11 <sub>ax</sub>	6 6, 7, 8	8, 11 <sub>eq</sub> 6, 11 <sub>ax</sub>
12	168.8 C				
13	120.1 CH	6.45, d, 15.0	14, 15, 16, 17	12, 15	6, 15, 16
14	142.1 CH	7.24, dd, 10.6, 15.0	13, 15	12, 16	16
15	132.0 CH	6.36, dd, 10.6, 15.0	14, 16		13, 14, 16, 17
16	139.3 CH	6.25, dq, 15.0, 6.5	13, 15, 17	14, 17	14, 17
17	18.8 CH <sub>3</sub>	1.85, d, 6.5	15, 16	15, 16	15, 16
18	11.0 CH <sub>3</sub>	1.09, s		2, 4, 8	8, 9 <sub>ax</sub>
19	26.9 CH <sub>3</sub>	1.14, s	6	2, 4, 5, 6	6
20	67.4 CH <sub>2</sub>	3.29, s		10	

Table 5. NMR-Spectral data of **4** measured in [D<sub>6</sub>]acetone at 300 and 500 MHz.

Position	$\delta_C$ in ppm	$\delta_H$ in ppm, mult., $J$ (Hz)	$^1H$ - $^1H$ COSY correlations	HMBC correlations	NOE correlations
1	107.8 C				
2	198.9 C				
3	64.7 C				
4	202.3 C				
5	74.5 C				
6	47.6 CH	3.74, d, 3.7	7	1, 2, 4, 5, 7, 8, 12	13, 19
7	80.9 CH	5.57, dd, 3.7, 10.6	6, 8	1, 3	
8	53.0 CH	3.58, dd, 2.9, 10.6	7, 9	2, 3, 4, 6, 9	9, 18
9	109.6 CH	5.75, d, 2.9	8	7, 8, 10, 11	8, 18
10	151.7 C				
11	161.0 C				
12	170.9 C				
13	120.2 CH	6.55, d, 15.0	14, 15, 16	1, 12, 15	6, 15, 17
14	143.4 CH	7.29, dd, 11.0, 15.0	13, 15	12, 16	16
15	132.6 CH	6.44 dd, 11.0, 15.0	14, 16	16, 17	13, 17
16	140.1 CH	6.26, dq, 15.0, 7.0	13, 15, 17	15, 17	14, 17
17	19.2 CH <sub>3</sub>	1.88, d, 7.0	15, 16	15, 16	15
18	10.6 CH <sub>3</sub>	1.19, s		2, 3, 4, 8	8, 9
19	23.9 CH <sub>3</sub>	1.25, s		4, 5, 6	6

and  $^{13}C$  NMR spectroscopic data see Table 3. EIMS:  $m/z$  (% rel. int.) = 408 (22) [M<sup>+</sup>], 376 (80), 359 (50), 305 (20), 287 (28), 101 (82), 95 (70), 59 (76), accurate mass found  $m/z$  408.1780 (calcd. for C<sub>21</sub>H<sub>28</sub>O<sub>8</sub>  $m/z$  408.1783).

**Trichdermanone C (3):** (11.9 mg); yellowish viscous oil.  $[a]_D^{22} = +265.7$  (MeOH,  $c = 0.5$ ). UV (MeOH)  $\lambda_{max}$  (log  $\epsilon$ ): 360 (4.3), 248 (3.8) nm. CD (MeOH)  $\Delta\epsilon = 333$  (+11.678), 297 (−10.631). IR (film):  $\tilde{\nu} = 3330, 2937, 1731, 1627, 1597, 1556, 1380$  cm<sup>−1</sup>.  $^1H$  and  $^{13}C$  NMR spectroscopic data see Table 4. EIMS:  $m/z$  (% rel. int.) = 394 (20) [M<sup>+</sup>], 376 (100), 305 (22), 287 (20), 101 (37), 95 (65), 59 (37), accurate mass found  $m/z$  394.1625 (calcd. for C<sub>20</sub>H<sub>26</sub>O<sub>8</sub>  $m/z$  394.1628).

**Trichodermanone D (4):** (2.0 mg); yellowish viscous oil.  $[a]_D^{22} = +51.5$  (MeOH,  $c = 0.08$ ). UV (MeOH)  $\lambda_{max}$  (log  $\epsilon$ ): 360 (4.3), 250 (4.2), 204 (4.1) nm. IR (film):  $\tilde{\nu} = 3383, 2923, 2359, 1729, 1599, 1404$  cm<sup>−1</sup>.  $^1H$  and  $^{13}C$  NMR spectroscopic data see Table 5. ES-IMS: positive ion  $m/z = 361$  [M + H<sup>+</sup>], negative ion  $m/z$  359 [M − H<sup>+</sup>]; accurate mass found  $m/z$  360.1209 (calcd. for C<sub>19</sub>H<sub>20</sub>O<sub>7</sub>  $m/z$  360.1209).

## Acknowledgments

The authors wish to thank Prof. Gerhard Raabe, RWTH Aachen, for the measurement of the CD spectra. This project is part of the Graduiertenkolleg GRK677 "Struktur und molekulare Interaktion als Basis der Arzneimittelwirkung" and is financially supported by the Deutsche Forschungsgemeinschaft (DFG).

- [1] G. M. König, A. D. Wright, *Planta Med.* **1996**, 62, 193–211.
- [2] G. M. König, A. D. Wright, *Trends in marine biotechnology in: Drug Discovery from Nature* (Eds.: S. Grabley, R. Thiericke), Springer Verlag, Berlin, **1999**, p. 180–187.
- [3] U. Höller, A. D. Wright, G. F. Matthée, G. M. König, S. Dräger, H.-J. Aust, B. Schulz, *Mycol. Res.* **2000**, 104, 1354–1365.
- [4] G. M. König, S. Kehraus, S. F. Seibert, A. Abdel-Lateff, D. Müller, *ChemBioChem* **2006**, 7, 229–238.
- [5] R. Andrade, W. A. Ayer, P. P. Mebe, *Can. J. Chem.* **1992**, 70, 2526–2535.
- [6] S. Sperry, G. J. Samuels, P. Crews, *J. Org. Chem.* **1998**, 63, 10011–10014.
- [7] H. G. Cutler, S. J. Cutler, S. A. Ross, K. El Sayed, F. M. Dugan, M. G. Barlett, A. A. Hill, R. A. Hill, S. R. Parker, *J. Nat. Prod.* **1999**, 62, 137–139.
- [8] F. A. Macias, R. M. Varela, A. M. Simonet, H. G. Culter, S. J. Culter, M. A. Eden, A. A. Hill, R. A. Hill, *J. Nat. Prod.* **2000**, 63, 1197–1200.
- [9] T. Matsumoto, A. Ishiyama, Y. Yamaguchi, R. Masuma, H. Ui, K. Shiomi, H. Yamada, S. Omura, *J. Antibiot.* **1999**, 52, 754–757.
- [10] L. Trifonov, J. H. Bieri, R. Prew, A. S. Dreiding, D. M. Rast, L. Hoesch, *Tetrahedron* **1982**, 38, 397–403.
- [11] N. Abe, T. Murata, A. Hirota, *Biosci. Biotechnol. Biochem.* **1998**, 62, 661–666.
- [12] L. S. Trifonov, H. Hilpert, P. Floesheim, A. S. Dreiding, D. M. Rast, R. Skrivanova, L. Hoesch, *Tetrahedron* **1986**, 42, 3157–3179.
- [13] R. P. Maskey, I. Grün-Wollny, H. Laatsch, *J. Nat. Prod.* **2005**, 68, 865–870.
- [14] N. Abe, O. Sugimoto, K. Tanji, A. Hirota, *J. Am. Chem. Soc.* **2000**, 122, 12606–12607.
- [15] D. Barnes-Seeman, E. J. Corey, *Org. Lett.* **1999**, 9, 1503–1504.
- [16] N. Abe, T. Murata, K. Yamamoto, A. Hirota, *Tetrahedron Lett.* **1999**, 40, 5203–5206.
- [17] G. Bringmann, G. Lang, T. A. M. Gulder, H. Tsuruta, J. Mühlbacher, K. Maksimenka, S. Steffens, K. Schaumann, R. Stöhr, J. Wiese, J. F. Imhoff, S. Perović-Ottstadt, O. Boreiko, W. E. G. Müller, *Tetrahedron* **2005**, 61, 7252–7265.
- [18] *ACD/Chem. Sketch*; ACD/Labs release: 9.00; Product Version: 9.08.
- [19] M. Karplus, *J. Am. Chem. Soc.* **1963**, 85, 2870–2871.
- [20] C. A. G. Haasnot, F. A. A. M. de Leeuw, C. Altona, *Tetrahedron* **1980**, 36, 2783–2792.
- [21] <http://www.casper.organ.su.se/ke3690/jhh.html>.
- [22] K. C. Nicolaou, K. B. Simonsen, G. Vassilikogiannakis, P. S. Baran, V. P. Vidali, E. N. Pitsinos, E. A. Couladouros, *Angew. Chem.* **1999**, 111, 3762–3766.
- [23] K. C. Nicolaou, G. Vassilikogiannakis, K. B. Simonsen, P. S. Baran, Y.-L. Zhong, V. P. Vidali, E. N. Pitsinos, E. A. Couladouros, *J. Am. Chem. Soc.* **2000**, 122, 3071–3079.
- [24] N. Abe, O. Sugimoto, T. Arakawa, K.-I. Tanji, A. Hirota, *Biosci. Biotechnol. Biochem.* **2001**, 65, 2271–2279.
- [25] J. M. A. Al-Rawi, J. A. Elvidge, D. K. Jaiswal, J. R. Jones, R. Thomas, *J. Chem. Soc., Chem. Commun.* **1974**, 220–221.

Received: December 18, 2006  
Published Online: March 23, 2007